Timescale for equilibration of N/Z gradients in dinuclear systems

K. Brown,[1] S. Hudan,[1,*] R. T. de Souza,[1,†] J. Gauthier,[2] R. Roy,[2] D. V. Shetty,[3] G. A. Souliotis,[3,4] and S. J. Yennello[3]

[1] *Department of Chemistry and Center for Exploration of Energy and Matter 2401 Milo B. Sampson Lane, Bloomington IN 47405, USA*

[2] *Université Laval, Québec, Canada*

[3] *Cyclotron Institute, Texas A&M University, College Station, TX 77843, USA*

[4] *Laboratory of Physical Chemistry, Department of Chemistry, National and Kapodistrian University of Athens, Athens 15771, Greece*

(Dated: September 20, 2018)

Equilibration of N/Z in binary breakup of an excited and transiently deformed projectile-like fragment (PLF*), produced in peripheral collisions of ^{64}Zn + ^{27}Al, ^{64}Zn, ^{209}Bi at E/A = 45 MeV, is examined. The composition of emitted light fragments (3≤Z≤6) changes with the decay angle of the PLF*. The most neutron-rich fragments observed are associated with a small rotation angle. A clear target dependence is observed with the largest initial N/Z correlated with the heavy, neutron-rich target. Using the rotation angle as a clock, we deduce that N/Z equilibration persists for times as long as 3-4 zs (1zs = 1 x 10^{-21}s = 300 fm/c). The rate of N/Z equilibration is found to depend on the initial neutron gradient within the PLF*.

PACS numbers: 25.70.Mn, 25.70.Lm

The broad impact of the density dependence of the nuclear symmetry energy makes it a topic of considerable interest. Whether the asymmetry term in the nuclear equation of state follows a stiff or a soft dependence on density determines the composition of a neutron star's crust, and the conditions under which a supernova explosion occurs [1–3]. In the case of nuclei, the stability of the heaviest elements [4], and the existence of neutron skins [5], also depend on this quantity. One means of investigating the density dependence of the symmetry energy is by measuring the N/Z equilibration in a dinuclear system [6–8]. Although past studies have principally focused on the N/Z equilibration that occurs between the projectile and target nuclei in a collision, such an approach is fundamentally limited by the short contact time between the two collision partners. This contact time, which is approximately 100 fm/c at intermediate energies, inherently limits the degree of equilibration that can be attained.

Another opportunity to investigate N/Z equilibration is the dynamical binary breakup of an excited and transiently deformed nucleus produced in the semi-peripheral collision of two heavy-ions at intermediate energies (E/A=20-100 MeV) [9]. At these energies, the collision of two heavy-ions at peripheral and mid-central impact parameters leads to the exchange of charge, mass, and energy between the projectile and target nuclei. Prior experimental and theoretical work demonstrates that several mechanisms can contribute to the ternary breakup of the transient system into two heavy remnants (projectile and target) together with one intermediate mass fragment [9–12]. For many such breakups, the existence of a short-lived neck joining the projectile and target plays a crucial role. As the two heavy remnants separate the neck ruptures leaving it still attached to one of the two remnants. The binary system consisting of the neck and associated remnant continues to undergo neutron and proton exchange as it rotates. If the neck is associated with the projectile remnant, we designate the joint neck-heavy remnant system as the projectile-like fragment (PLF*). In the case of ternary decays a second rupture of the neck occurs producing the intermediate mass fragment. Statistical decay from the equilibrated projectile and target remnants also occurs.

Equilibration of N/Z within the PLF* has been observed to persist for timescales as long as t ≈ 3zs (1zs = 1 x 10^{-21}s) [13]. In the present work we further characterize this approach, extending it to a significantly lighter projectile. We explore the impact of the N/Z of the target on the composition of the fragments produced and their subsequent evolution. We also demonstrate that this equilibration process exists when the projectile and target nuclei are the same nucleus.

The experiment was conducted at the Cyclotron Institute at Texas A&M University, where a beam of ^{64}Zn ions was accelerated to E/A = 45 MeV with an average beam intensity of ≈2x10^8 p/s. The beam impinged on ^{27}Al, ^{64}Zn and ^{209}Bi targets with thicknesses of 13.4, 5, and 1 mg/cm^2 respectively. Although the experimental details have been previously published [14], they are summarized below for completeness. The array FIRST [15],which subtended the angular range 4.5° ≤ θ_{lab} ≤ 27° was used to identify charged products produced in the reaction. In the angular range 4.5° ≤ θ_{lab} ≤ 7°, the forward telescope in FIRST provided identification by atomic number of all products up to Z=30 and isotopic information for Z ≤ 12. The second telescope in FIRST

*Electronic address: shudan@indiana.edu
†Electronic address: desouza@indiana.edu

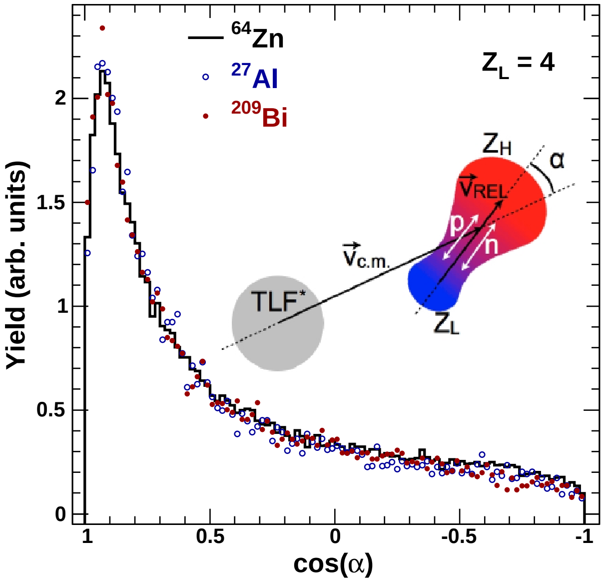

FIG. 1: (Color online) The angular distribution of binary splits (Z_L-Z_H) for Z_L=4, representative of other fragments, is shown. Data for the ^{64}Zn, ^{27}Al, and ^{209}Bi targets are represented by the black line, blue open symbol and red closed symbol histograms respectively.

, which subtended the angular range $7° \leq \theta_{lab} \leq 14°$, provided Z identification for Z ≤ 22 and A identification for Z ≤ 8. The third telescope in FIRST ($14° \leq \theta_{lab} \leq 27°$) provided Z identification for Z ≤ 12 and A identification for Z ≤ 7. The high segmentation of FIRST provided an angular resolution of ±0.05°($4.5° \leq \theta_{lab} \leq 7°$), ±0.44°($7° \leq \theta_{lab} \leq 14°$) and ±0.81°($14° \leq \theta_{lab} \leq 27°$) in polar angle and ±11.25° in azimuthal angle. The energy resolution obtained was approximately 1%.

In order to focus on binary decays, events were selected in which two fragments (Z ≥ 3) were detected within the laboratory angular range $4.5° \leq \theta_{lab} \leq 27°$. These two fragments were distinguished from each other by their atomic number, with the larger (smaller) atomic fragment designated as Z_H (Z_L). We ensured that the PLF* under investigation comprised a large fraction of the initial projectile by requiring that the events selected had $Z_H > 11$. Events selected in this manner corresponded to approximately 14% of the measured yield in which one fragment with Z>11 was detected.

It has previously been established that an instructive quantity for the binary decay of the PLF* is the angle between the direction of the two fragments center-of-mass velocity, $v_{c.m.}$, and their relative velocity, v_{REL}, defined as v_H-v_L [16, 17]. We construct the angle α, with

$$cos(\alpha) = v_{c.m.} \cdot v_{REL}/(\|v_{c.m.}\|\|v_{REL}\|)$$

as indicated within the inset of Fig. 1. Consequently, aligned decays with Z_L emitted backward (forward) of Z_H corresponds to cos(α) = 1 (-1). Momentum correlations observed between Z_H and Z_L reveal that these two fragments originate from a common parent as evident in Fig. 2 of [17]. This parent nuclear system comprised of Z_H and Z_L is designated as the PLF*.

The angular distribution for Z_L=4 fragments is presented in Fig. 1 for the ^{64}Zn, ^{27}Al, and ^{209}Bi targets used. Consistent with previous work, all the angular distributions manifest a peak at backward angles cos(α)>0.5. This preferential backward decay of the PLF* is well established, and has been interpreted as the aligned dynamical decay of the excited and transiently deformed PLF* [16, 18, 19]. The backward peaking of the angular distribution can be understood as the dynamical binary splitting of the PLF* on a timescale that is short relative to the rotational period of the PLF*. To compare the shape for the different targets, all three distributions have been normalized in the interval -1≤cos(α)<0. We chose this region for normalization since it corresponds to forward statistical emission from the PLF*. This forward statistical decay is long-lived relative to backward emission and hence is less coupled to any dynamics responsible for the formation of the PLF*. For each target, the angular distributions exhibit the same shape, manifesting a distinct preference for aligned decay of the PLF* with the Z_L fragment oriented towards the target. The shape of the distribution for cos(α)<0 provides an indication that the angular momentum of the decaying PLF* is relatively small. In contrast to previously studied systems [13], the yield does not increase near cos(α)=-1.

Given the normalization at forward angles, the similarity of the distributions for the three targets at backward angles, cos(α)>0, is striking. This similarity suggests that while the probability of forming the elongated and excited PLF*, as well as its composition, may depend on the target, the relative probability of its subsequent decay is essentially independent of the target.

We next examine whether the composition of the Z_L fragment changes as a function of rotation angle. In our initial work, which analyzed the reaction ^{124}Xe + ^{112,124}Sn, we observed that the ⟨N⟩/Z of the Z_L fragment decreased as the Z_L-Z_H system rotated [13]. As the Zn-like PLF* in the present work is considerably smaller than the Xe-like PLF*, it was unclear whether the behavior previously observed would also exist for the smaller PLF*. Depicted in Fig. 2 is the ⟨N⟩/Z of the Z_L fragment for Be (panel a), B (panel b), and C (panel c) fragments. For each Z_L shown the impact of the three different targets is also presented. The average ⟨N⟩/Z for a given Z_L is deduced by averaging the neutron number for the different isotopes measured. A common feature of all the data is that the largest value of ⟨N⟩/Z is associated with cos(α)=1, namely backward emission. As the Z_L-Z_H system rotates, ⟨N⟩/Z of the Z_L fragment decreases corresponding to a net loss of neutrons by the Z_L fragment. In the case of the Be fragments, this dependence of ⟨N⟩/Z on cos(α) is clearly apparent even for the lightest target, Al. For all three fragments shown the magnitude of ⟨N⟩/Z is largest for the Bi target. We attribute this large value of ⟨N⟩/Z for cos(α)≈1 in the case of the Bi target to the preferential pickup of neutrons by the PLF* from the Bi target with its N/Z=1.51. In contrast, the

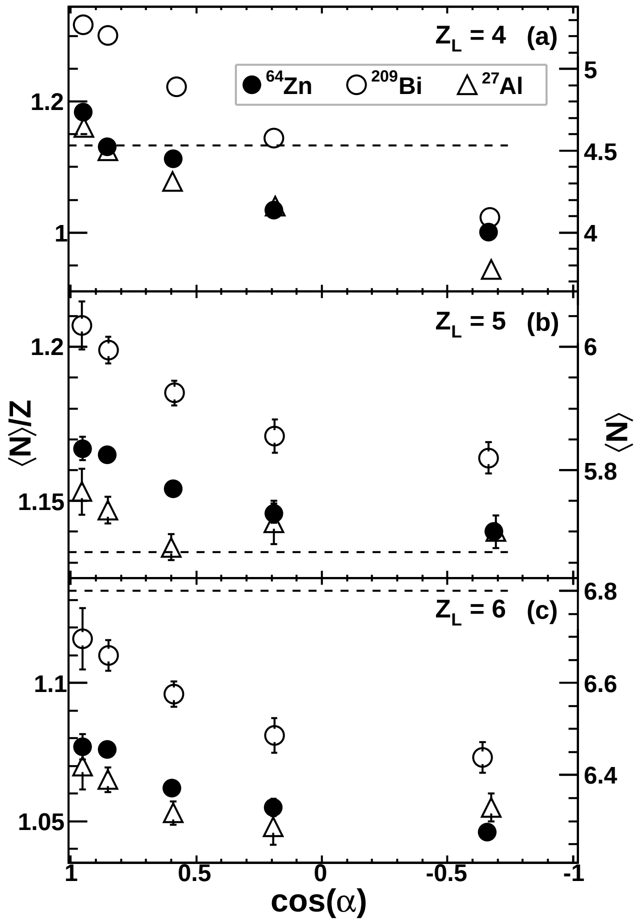

FIG. 2: Average neutron to proton ratio for selected Z_L as a function of the decay angle. The ratio for the ^{64}Zn, ^{209}Bi, and ^{27}Al targets is represented by the closed circle, open circle and open triangle respectively. The dashed line for each Z_L represents the N/Z of the ^{64}Zn beam.

^{64}Zn and ^{27}Al targets with N/Z = 1.13 and 1.07 do not present a neutron-rich reservoir from which the PLF* can pick up neutrons.

Shown in the right hand scale of Fig. 2 is the ⟨N⟩ of the Z_L fragment. In the case of the Be fragments, for the Bi target ⟨N⟩ decreases from 5.2 to 4.05 a net change of over one neutron. For the Zn and Al targets, a somewhat smaller net decrease of 0.6 - 0.7 in neutron number is observed. For the Bi target, the change in ⟨N⟩ for Z_L=5 and Z_L=6 is ≈0.2. The change in ⟨N⟩ for Li fragments and the Bi target (not shown) is also ≈0.2, comparable to that of B and C fragments. The larger change observed in the case of Be fragments can be qualitatively understood as being due to the absence of ^{8}Be fragments. Since the isotopic distribution for all the fragments with Z_L=3,5, and 6 has a value of ⟨N⟩/Z>1, it is reasonable to expect that this is also the case for Be fragments. The decay of ^{8}Be into two alpha particles removes these fragments from the measured isotopic distribution thus artificially increases the value of ⟨N⟩ observed for Be at backward angles. In effect, the absence of ^{8}Be acts as an amplifier for the change in ⟨N⟩ by emphasizing the importance of the extremes of the isotopic distribution. This conclusion is supported by our re-analysis of carbon isotopes in which we eliminate ^{12}C from the isotopic distribution[20]. For this reason, we have elected to present the Be data without correcting for the absence of ^{8}Be.

The physical picture that emerges is one in which the N/Z of the dinuclear PLF* is established through its interaction with the target. Preferential transfer of neutrons from a neutron-rich target such as Bi results in a neutron-rich PLF*. As the nascent Z_L fragment is oriented towards the target-like fragment, it is the primary beneficiary of the transferred neutrons. In addition, even for a symmetric projectile-target collision, the density dependence of the symmetry energy leads to neutron enrichment of the low-density neck[14]. The result is an initial N/Z gradient within the PLF*. As time passes, these additional neutrons in the Z_L fragment are dissipated. Whether this preferential neutron transport out of the Z_L fragment occurs into the Z_H fragment or into a low-density neck region connecting the Z_L and Z_H fragments is presently unclear [12]. It should be clear that transfer of both neutrons and protons occurs between the Z_H and Z_L fragments. Our selection of a particular Z_L fragment in this analysis precludes us from examining the net proton exchange.

If the decrease in ⟨N⟩/Z with cos(α) can be understood as the preferential transport of neutrons out of the Z_L fragment, one might expect that the shorter the contact time between the Z_L and Z_H fragments the less likely it is that the initial ⟨N⟩/Z is decreased. Dynamical splitting of the dinuclear Z_H-Z_L system can be viewed as a dynamical fission process in which the reaction dynamics provides collective motion along the separation axis of the Z_L-Z_H system [11, 16, 17]. Within such a picture we expect that the shortest times (dynamical ruptures) are associated with the largest relative velocities and the longest times are associated with smallest (Coulomb barrier) relative velocities.

In order to explore the dependence of ⟨N⟩/Z on both cos(α) and v_{REL}, we present the dependence of ⟨N⟩ of Be fragments in velocity space in Fig. 3. In this figure, the dependence of the average neutron number, ⟨N⟩, of Be fragments on the transverse ($v_{REL,\perp}$) and parallel ($v_{REL,\parallel}$) components of v_{REL} is depicted. The parallel and transverse components of v_{REL} are calculated with respect to the center-of-mass velocity of the Z_L-Z_H system. For reference, relative velocities between 1.5 and 5.5 cm/ns are indicated as dotted circles while the angular cuts over which the average neutron number was calculated are represented by dashed lines.

For the ^{209}Bi (panel a) target a systematic behavior of ⟨N⟩ of the Be fragment is observed. As one rotates clockwise in the two dimensional velocity space, i.e. increasing rotation angle α, the value of ⟨N⟩ decreases. For the largest v_{REL}, the ⟨N⟩ of the Z_L fragment decreases from 5.5 to 4.46, a change of ≈ 1 neutron as the Z_H-Z_L system rotates by a quarter turn. For the two most backward an-

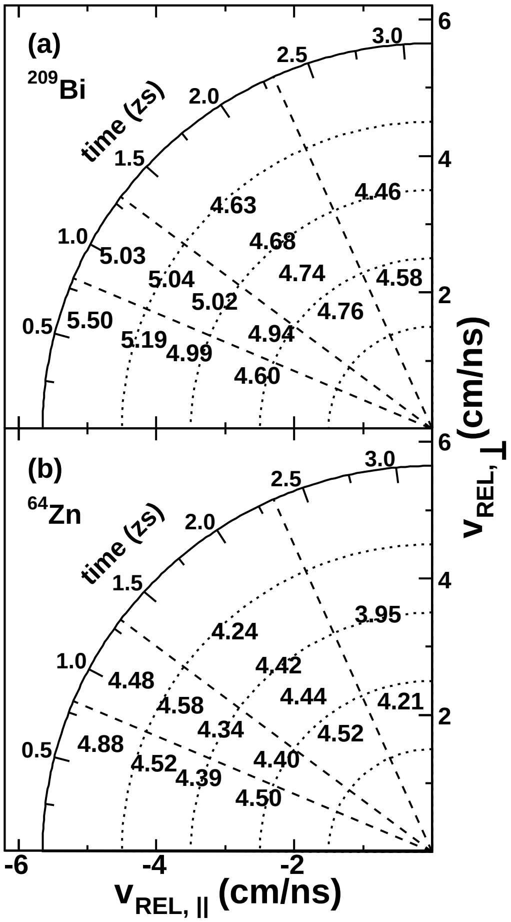

FIG. 3: Dependence of the average neutron number on the parallel and transverse components of v_{REL} for $Z_L = 4$ for the reactions ^{64}Zn + ^{209}Bi, ^{64}Zn.(See text for details)

gle bins one observes that ⟨N⟩ decreases with decreasing $v_{REL,\parallel}$ (from 5.5 to 4.6), while for larger rotation angles, ⟨N⟩ increases with decreasing $v_{REL,\parallel}$ (from 4.46 to 4.58). From this trend, one would predict that ⟨N⟩ and hence ⟨N⟩/Z would decrease with increasing v_{REL} for forward emission. This expectation is confirmed for this system in agreement with previous observation [13]. These trends are also observed for the ^{64}Zn (panel b) target although the magnitude of the change is slightly smaller than in the ^{209}Bi case.

To extract the time dependence of the ⟨N⟩ of the Z_L fragment, we utilize the rotation angle of the Z_L-Z_H dinuclear system as a clock such that the rotation time, t is given by: $t = \alpha/\omega$ where ω is the angular frequency. Hence, the quantity to be determined is the angular frequency which is given by: $\omega = (J\hbar)/I_{eff}$ where J is the angular momentum and I_{eff} is the moment of inertia for the dinuclear system. The angular momentum of the dinuclear complex is determined by utilizing a simple model that describes the statistical decay of a rotating system, appropriate for forward emission. This model was chosen because it provides a simple way to include the effects of thermal excitation and collective rotation but may have some limitations. The magnitude and direction of the velocity of the PLF* are determined by sampling the experimental data for forward emission. The magnitude of the relative velocity vector between Z_H and Z_L is taken from the Viola systematics [21] with a width provided from the experimental data. The in-plane and out-of-plane components of v_{REL} are calculated relative to the plane defined by the PLF* and beam direction. The distribution of the out-of-plane emission of Z_L is taken as: P(sinϕ)=Aexp(-$k^2 sin^2\phi$) where ϕ is the out-of-plane angle, k represents the width of the distribution, and A is a normalization constant. The model predictions have been filtered by the detector acceptance and compared to the experimentally measured angular distributions presented in Fig. 1. Comparison of the measured and predicted distributions for different values of k indicates that the magnitude of k is ≈ 0.5. Within the framework of a fissioning nucleus, the parameter k can be related to angular momentum [22]: $J^2 = (2k^2 I_{eff} T)/\hbar^2$ where T is the temperature and I_{eff} is calculated as: $I_{eff} = \frac{2}{5} MR^2 F_I$. The mass, M, is approximated as: $M = m_0 c^2 A_{PLF^*}$ where m_0c^2 is the rest mass of the nucleon and $A_{PLF^*} = \left(\frac{A}{Z}\right)_{projectile} Z_{PLF^*}$. The effective radius of the dinuclear configuration is given by R^2F_I with $R=r_0A^{1/3}$ and the deviation from a sphere accounted for by F_I [23]. The value of the radius constant r_0 is taken as 1.2 fm. As F_I has not been calculated for a system as light as the PLF* under consideration, we use the published value for the significantly heavier nucleus, ^{149}Tb [23]. Assuming a temperature of T=3-5 MeV for the system undergoing binary decay, we calculate an angular momentum J=6±1 $\hbar$.

The timescale deduced in this manner is shown in Fig. 3. It should be noted that the timescale deduced (t ≤ 3 zs) is consistent with previously published results [13, 24, 25]. For reference, the angular velocity calculated for this light dinuclear complex is 0.4-0.5 x 10^{21}rad/sec.

Having associated the rotation angle with a timescale, it is now possible to observe two timescales evident in Fig. 3. The first observation is that for this system even for times as long as 3 zs, i.e. 900 fm/c, the ⟨N⟩ of the Z_L fragment is still changing indicating that N/Z equilibration is a slow process. In addition, operating on a faster timescale of ≈ 1 zs, the v_{REL} dependence observed for the most backward angles is overpowered by the Coulomb effect that characterizes forward emission [26]. The pattern observed for Z_L=4 in Fig. 3 indicates that even for backward angles a correlation exists between the rotation angle dependence and the v_{REL} dependence for ⟨N⟩. However, disentangling the intrinsic N/Z gradient from the Coulomb contribution at backward angles requires knowledge of the detailed configuration of the dinuclear system. The trajectory of the Z_L fragment depends on the motion of the Z_L fragment relative to both the target-like and Z_H fragments which perturbs the intrinsic N/Z pattern. This disentanglement is beyond the scope of the present work. We therefore examine the dependence of

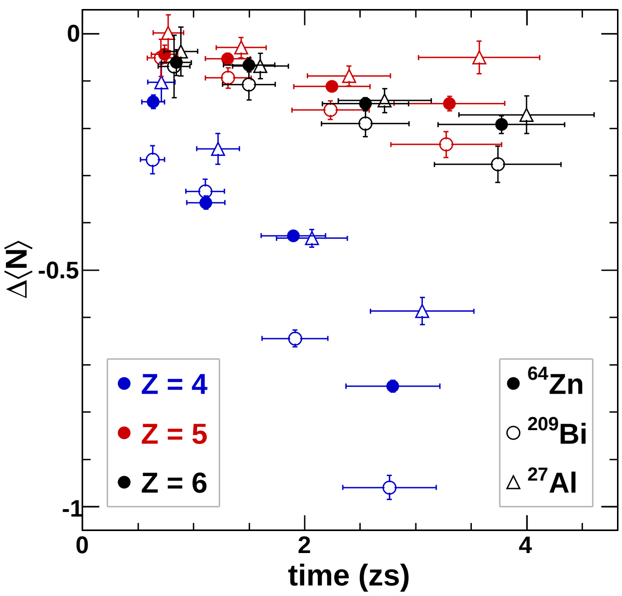

FIG. 4: (Color online) Dependence of the average differential neutron number on time for Z_L = 4, 5 and 6 for the reactions ^{64}Zn + ^{64}Zn, ^{209}Bi and ^{27}Al.(See text for details)

⟨N⟩ on time, integrated over v_{REL}.

Shown in Fig. 4 is the time dependence of ⟨N⟩ for Z_L=4, 5, and 6 fragments. To compare the change in ⟨N⟩ for different targets and different Z_L fragments, we subtracted the extrapolated value of ⟨N⟩ at t=0. This extrapolated value was determined by performing a linear fit of ⟨N⟩ versus time. It is interesting that the data shown in Fig. 4 clearly fall into two groups. While Z_L=4 exhibits a strong dependence of Δ⟨N⟩ on time, Z_L=5 and 6 fragments manifest a much weaker dependence. In the case of Z_L=4 fragments, a strong and clear target dependence is evident. Close examination of the data for Z_L=5 and 6 fragments reveals that the same target dependence exists though it is smaller in magnitude. For Z_L = 4, the Bi target is associated with the largest change in ⟨N⟩, ≈1. The Zn and Al targets exhibit smaller changes of 0.75 and 0.6 respectively. The horizontal error bars shown in the figure are primarily governed by an estimated uncertainty of ΔJ=1ħ. It should be noted that the magnitude of the change in ⟨N⟩ is considerably larger than that previously reported for the Xe + Sn system [13].

For Be fragments the large slope of Δ⟨N⟩ versus time indicates significant equilibration occurs on the timescale of 3 zs. One can imagine that the rate of equilibration is governed by the initial difference in N/Z between the Z_L and Z_H fragments, i.e. a gradient in N/Z within the PLF*. Confirming this perspective is the behavior of Be fragments for different targets. The data for the Bi target manifests the largest slope and the one for the Al target the smallest slope corresponding directly to the neutron-enrichment of the Z_L fragment as evident in Fig. 2. This target dependence suggests a fundamental result. The neutrons transferred from the target do *not* equilibrate within the PLF* prior to it attaining the dinuclear configuration. If they did, all three targets would manifest the same equilibration rate. Thus the experimental data directly indicate that the equilibration rate of ⟨N⟩ is governed by the initial N/Z gradient in the dinuclear system.

In summary, to investigate the N/Z equilibration timescale for a dinuclear complex, we have focused on the binary decay of a PLF*. For this system, we have shown that the isotopic composition (⟨N⟩/Z) of the fragments depends on the rotation angle of the dinuclear complex. Moreover, the N/Z of the Z_L fragment depends on the neutron-richness of the target. While we observe these effects for Z_L=4, 5, and 6 fragments, they are strongest in the case of Be fragments. This large magnitude for Be fragments can be qualitatively understood as due to the absence of ^{8}Be in the isotopic distribution making Be a sensitive probe of the equilibration process. Within our analysis, the N/Z equilibration is related to the change in average neutron number, Δ⟨N⟩, experienced by the Z_L fragment. Using the rotation angle of the dinuclear complex we deduce the timescale on which the N/Z equilibration occurs. The equilibration persists for as long as 3-4 zs. Clear evidence for a target dependence of the equilibration rate is observed in the case of Be fragments. The largest equilibration rate (Bi target) is associated with the largest initial neutron-enrichment of the Z_L fragment. These differences in equilibration rate can be related to different initial N/Z gradients within the dinuclear configuration for the different targets. While qualitatively the physical picture associated with these observations is clear, a more detailed understanding of the N/Z equilibration will require comparison with a theoretical model that describes nucleon transport within the dinuclear complex.

Acknowledgments

This work was supported by the U.S. Department of Energy under Grant Nos. DEFG02-88ER-40404 (IU) and DE-FG03-93ER40773 (TAMU). Support from the Robert A. Welch Foundation through Grant No. A-1266 is gratefully acknowledged. Collaboration members from Université Laval recognize the support of the Natural Sciences and Engineering Research Council of Canada.

[1] J. Lattimer and M. Prakash, Astrophys. J. **550**, 426 (2001).
[2] A. Steiner et al., Phys. Rep. **411**, 325 (2005).
[3] H. T. Janka et al., Phys. Rep. **442**, 38 (2007).
[4] P. Möller et al., Phys. Rev. Lett. **108**, 052501 (2012).
[5] M. B. Tsang et al., Phys. Rev. C **86**, 015803 (2012).

[6] M. B. Tsang et al., Phys. Rev. Lett. **92**, 062701 (2004).
[7] A. L. Keksis et al., Phys. Rev. C **81**, 054602 (2010).
[8] Z. Kohley et al., Phys. Rev. C **86**, 044605 (2012).
[9] E. D. Filippo et al., Phys. Rev. C **86**, 014610 (2012).
[10] C. P. Montoya et al., Phys. Rev. Lett. **73**, 3070 (1994).
[11] J. Colin et al., Phys. Rev. C **67**, 064603 (2003).
[12] V. Baran et al., Phys. Rev. C **85**, 054611 (2012).
[13] S. Hudan et al., Phys. Rev. C **86**, 021603(R) (2012).
[14] D. Thériault et al., Phys. Rev. C **74**, 051602 (R) (2006).
[15] T. Paduszynski et al., Nucl. Instr.and Meth. A **547**, 464 (2005).
[16] B. Davin et al., Phys. Rev. C. **65**, 064614 (2002).
[17] A. B. McIntosh et al., Phys. Rev. C **81**, 034603 (2010).
[18] P. Glässel et al., Z. Phys. A **310**, 189 (1983).
[19] J. Lecolley et al., Phys. Lett. B **354**, 202 (1995).
[20] See Supplemental Material at [URL will be inserted by publisher] for an assessment of the impact of the missing ^{8}Be.
[21] V. Viola et al., Phys. Rev. C **31**, 1550 (1985).
[22] R. Vandenbosch and J. R. Huizenga, *Nuclear Fission* (Academic Press, 1973).
[23] N. Carjan and M. Kaplan, Phys. Rev. C **45**, 2185 (1992).
[24] G. Casini et al., Phys. Rev. Lett. **71**, 2567 (1993).
[25] S. Piantelli et al., Phys. Rev. Lett. **88**, 052701 (2002).
[26] S. Hudan et al., Phys. Rev. C **71**, 054604 (2005).